PHYSICAL REVIEW D **96**, 043503 (2017)

Can interacting dark energy solve the H_0 tension?

Eleonora Di Valentino,[1,2,*] Alessandro Melchiorri,[3,†] and Olga Mena[4,‡]

[1] *Institut d'Astrophysique de Paris (UMR7095: CNRS & UPMC-Sorbonne Universities), F-75014 Paris, France*

[2] *Sorbonne Universités, Institut Lagrange de Paris (ILP), F-75014 Paris, France*

[3] *Physics Department and INFN, Università di Roma "La Sapienza", Ple Aldo Moro 2, 00185 Rome, Italy*

[4] *IFIC, Universidad de Valencia-CSIC, 46071 Valencia, Spain*

(Received 11 May 2017; published 7 August 2017)

The answer is yes. We indeed find that interacting dark energy can alleviate the current tension on the value of the Hubble constant H_0 between the cosmic microwave background anisotropies constraints obtained from the Planck satellite and the recent direct measurements reported by Riess *et al.* 2016. The combination of these two data sets points toward a nonzero dark matter-dark energy coupling ξ at more than two standard deviations, with $\xi = -0.26^{+0.16}_{-0.12}$ at 95% C.L., i.e. with a moderate evidence for interacting dark energy with an odds ratio of 6:1 respect to a non interacting cosmological constant. However the H_0 tension is better solved when the equation of state of the interacting dark energy component is allowed to freely vary, with a phantomlike equation of state $w = -1.185 \pm 0.064$ (at 68% C.L.), ruling out the pure cosmological constant case, $w = -1$, again at more than two standard deviations. When Planck data are combined with external datasets, as BAO, JLA Supernovae Ia luminosity distances, cosmic shear or lensing data, we find perfect consistency with the cosmological constant scenario and no compelling evidence for a dark matter-dark energy coupling.

DOI: 10.1103/PhysRevD.96.043503

I. INTRODUCTION

The recent measurements of cosmic microwave background anisotropies (CMB) provided by the Planck satellite have fully confirmed the predictions of the standard cosmological model (hereafter, ΛCDM), based on cold dark matter, a cosmological constant, and inflation [1]. However, when constraints on the cosmological parameters of the ΛCDM model are derived from the Planck data, some tensions appear between their values and the corresponding values obtained from independent, complementary, observables.

The most important tension concerns the value of the Hubble constant. Indeed, the latest analysis of CMB temperature and polarization data from the Planck experiment provides the constraint of $H_0 = 66.93 \pm 0.62$ km/s/Mpc at 68% C.L., obtained assuming ΛCDM [2]. This is more than 3σ away from the recent direct and local determination of Riess *et al.* 2016 (R16, hereafter) of $H_0 = 73.24 \pm 1.74$ km/s/Mpc [3].

Another important discrepancy is present on the recovered values of the $S_8 = \sigma_8\sqrt{\Omega_m/0.3}$ parameter (where σ_8 is the amplitude of matter fluctuations and Ω_m is the matter density) derived independently by Planck and weak lensing surveys such as CFHTLenS [4,5] and KiDS-450 [6]. Considering a ΛCDM scenario, the KiDS-450 result is in tension with the Planck constraint at about 2.3 standard deviations (see e.g. [7]).

Clearly, unresolved systematics can still play a key role in explaining these discrepancies, however several physical mechanisms beyond ΛCDM that could change the derived values of H_0 and/or S_8 from Planck have been proposed, either solving or alleviating the tensions with the extracted values from R16 and cosmic shear local measurements (see e.g. Refs. [7–31]).

In this paper we focus our attention on dark energy: it has indeed been shown that introducing a dark energy equation of state (constant with time) $w < -1$ not only can solve the tension on the Hubble parameter but also does it in a more efficient way than other nonstandard extensions as, for example, the inclusion of extra relativistic degrees of freedom, via the $N_{\rm eff}$ parameter [9]. At the same time, a dynamical dark energy component seems to be favored in combined analyses of Planck and cosmic shear data (see e.g. [7]).

On top of that we should not forget that a cosmological constant clearly presents a puzzling and controversial solution to the dark energy problem, being probably the major theoretical weakness of the standard cosmological model. The possibility of having a different candidate for this component should be therefore investigated and any hints for deviations from the ΛCDM picture must be carefully scrutinized.

If the solution for the current tensions is within the dark energy sector then it is worthwhile to investigate which dark energy model is better suited for this task. Recently,

*eleonora.di_valentino@iap.fr
†alessandro.melchiorri@roma1.infn.it
‡omena@ific.uv.es

several authors have considered different parameterizations of the dark energy equation of state, deriving bounds arising from a number of cosmological data sets (see e.g. [16,32]). Here we focus on interacting dark matter-dark energy models. Indeed, a larger value for the Hubble parameter from CMB data can be obtained by including possible interactions between the dark energy and dark matter components (see e.g. [33–40]). More specifically, assuming the interacting dark energy model presented in Ref. [41], when considering the Planck 2013 data release, one gets the constraint $H_0 = 72.1^{+3.2}_{-2.3}$ km/s/Mpc at 68% C.L., that is significantly larger than the constraint $H_0 = 67.3 \pm 1.2$ km/s/Mpc at 68% C.L. obtained with the same data set but assuming a cosmological constant and no interaction (see Ref. [42]).

It is therefore timely to investigate if the same interacting dark energy model can also solve the tension between the new Planck 2015 data release (that includes new polarization data, which significantly improve the constraining power of these measurements) and the new bound R16, that in practice reduces by ∼42% the uncertainty of previous late-universe constraints on the Hubble constant [43].

In what follows we perform such an analysis, showing that indeed the current tension on H_0 can be solved by introducing an interaction between dark energy and dark matter as the one proposed by Ref. [41]. Moreover, it is also important to examine if the coupling can solve the tension *more efficiently* than a dark energy equation of state $w < -1$. For this reason we also perform an analysis by varying at the same time both the coupling and the equation of state of the dark energy component, as in interacting scenarios the dark energy equation of state of the dark matter fluid could in principle be different from that corresponding to the cosmological constant case.

Our work is organized as follows: in the following section we describe the interacting dark energy model assumed here, in Sec. III we describe the cosmological data and the analysis method and in Sec. IV we show the obtained results. Finally, we draw our conclusions in Sec. V.

II. INTERACTING DARK ENERGY

As previously stated, we consider the interacting dark energy scenario of Refs. [41,42], which can be parametrized as:

$$\nabla_\mu T^\mu_{(dm)\nu} = Q u_\nu^{(dm)}/a, \tag{1}$$

$$\nabla_\mu T^\mu_{(de)\nu} = -Q u_\nu^{(dm)}/a. \tag{2}$$

In the equations above, $T^\mu_{(dm)\nu}$ ($T^\mu_{(de)\nu}$) refers to the dark matter (dark energy) energy-momentum tensor, Q is the interaction rate and $u_\nu^{(dm)}$ is the four-velocity of the dark matter fluid. In order to avoid instabilities in the evolution of the linear perturbations, we restrict ourselves to the case in which Q reads as:

$$Q = \xi \mathcal{H} \rho_{de}, \tag{3}$$

i.e. the interaction rate is proportional to the dark energy density ρ_{de} via a dimensionless parameter ξ (that needs to be negative) and $\mathcal{H} = \dot{a}/a$, with the dot referring to derivative respect to conformal time.

The evolution equations for the interacting background read as [41]

$$\dot{\rho}_{dm} + 3\mathcal{H}\rho_{dm} = \xi \mathcal{H} \rho_{de}, \tag{4}$$

$$\dot{\rho}_{de} + 3\mathcal{H}(1+w)\rho_{de} = -\xi \mathcal{H} \rho_{de}. \tag{5}$$

The perturbation evolution, within the linear regime, and in the synchronous gauge, is given by [41]

$$\dot{\delta}_{dm} = -\left(k v_{dm} + \frac{1}{2}\dot{h}\right) + \xi \mathcal{H} \frac{\rho_{de}}{\rho_{dm}} (\delta_{de} - \delta_{dm}) + \xi \frac{\rho_{de}}{\rho_{dm}} \left(\frac{k v_T}{3} + \frac{\dot{h}}{6}\right), \tag{6}$$

$$\dot{\delta}_{de} = -(1+w)\left(k v_{de} + \frac{1}{2}\dot{h}\right) - 3\mathcal{H}(1-w) \times \left[\delta_{de} + \mathcal{H}(3(1+w)+\xi)\frac{v_{de}}{k}\right] - \xi\left(\frac{k v_T}{3} + \frac{\dot{h}}{6}\right), \tag{7}$$

$$\dot{v}_{dm} = -\mathcal{H} v_{dm}, \tag{8}$$

$$\dot{v}_{de} = 2\mathcal{H}\left(1 + \frac{\xi}{1+w}\right) v_{de} + \frac{k}{1+w}\delta_{de} - \xi \mathcal{H} \frac{v_{dm}}{1+w}, \tag{9}$$

with $\delta_{dm,de}$ and $v_{dm,de}$ the density perturbation and the velocity of the two fluids, v_T is the center of mass velocity for the total fluid and the dark energy speed of sound is $\hat{c}^2_{sde} = 1$. The equations above include the contributions of the perturbation in the expansion rate $H = \mathcal{H}/a + \delta H$.

Following Refs. [41,44,45], we have considered adiabatic initial conditions for all components. It has been shown there that, if one assumes adiabatic initial conditions for all the standard cosmological fluids (photon, baryons,…), the coupled dark energy fluid will also obey adiabatic initial conditions. In the synchronous gauge and at leading order in $x = k\tau$, the initial conditions read:

$$\delta_{de}^{\mathrm{in}}(x) = (1+w-2\xi)\frac{(1+w+\xi/3)}{12w^2-2w-3w\xi+7\xi-14} \times \left(\frac{-2\delta_\gamma^{\mathrm{in}}(x)}{1+w_\gamma}\right),$$

$$v_{de}^{\mathrm{in}} = \frac{x(1+w+\xi/3)}{12w^2-2w-3w\xi+7\xi-14}\left(\frac{-2\delta_\gamma^{\mathrm{in}}(x)}{1+w_\gamma}\right),$$

where $\delta_\gamma^{\mathrm{in}}(x)$ are the initial conditions for the photon density perturbations and $w_\gamma = 1/3$ is the equation of state of the photon, see Ref. [46] for the uncoupled case.

III. METHOD

The interacting dark energy scenario requires the six standard cosmological parameters of the ΛCDM plus one more parameter defined in the previous section, the coupling ξ. In particular, for the ΛCDM model, the parameters are the baryon density $\Omega_b h^2$, the cold dark matter density $\Omega_c h^2$, the reionization optical depth τ, and the ratio between the sound horizon and the angular diameter distance at decoupling θ_s. Furthermore, we consider two parameters directly related to the inflationary paradigm, that are the spectral index n_S and the logarithm of the amplitude of the primordial power spectrum, $\ln(10^{10}A_S)$. As a second step, we extend this baseline model, by adding one more parameter, a freely varying dark energy equation of state w, assumed to be constant in redshift.

We analyze this scenario by combining several cosmological probes. We consider the full temperature power spectrum provided by the Planck collaboration [47] at multipoles $2 \leq \ell \leq 2500$, in combination with the low-ℓ polarization power spectra in the multipoles range $2 \leq \ell \leq 29$. We refer to this combination as "Planck TT + lowTEB". We also include the high multipole Planck polarization spectra [47], in the multipole range $30 \leq \ell \leq 2500$. We refer to this combination as "Planck TTTEEE + lowTEB". However, we would like to recall here that this combination of data sets is considered less robust as it still under discussion due to some possible residual systematics contamination [1,47].

In addition to the CMB data sets described above, we consider their combination with the following cosmological measurements:

(i) tau055: We replace the "lowTEB" Planck data with a Gaussian prior on the reionization optical depth $\tau = 0.055 \pm 0.009$, as obtained from the Planck HFI measurements in [2];

(ii) lensing: We consider the 2015 Planck CMB lensing reconstruction power spectrum $C_\ell^{\phi\phi}$ obtained with the CMB trispectrum analysis [48];

(iii) BAO: Baryon acoustic oscillation measurements from the 6dFGS [49], SDSS-MGS [50], BOSSLOWZ and CMASS-DR11 [51] surveys are also considered;

(iv) R16: As previously stated, we include a Gaussian prior on the Hubble constant $H_0 = 73.24 \pm 1.74$ km/s/Mpc by quoting the value provided with direct measurements of luminosity distances in Riess *et al.* [3];

(v) JLA: We also employ luminosity distance data of Supernovae type Ia from the "Joint Light-curve Analysis" derived from the SNLS and SDSS catalogs [52];

(vi) WL: We add weak lensing galaxy data from the CFHTlens [4,5] survey with the priors and conservative cuts to the data as described in Ref. [1].

The analysis is done with a modified version of the most recent publicly available Monte-Carlo Markov Chain package COSMOMC [53], with a convergence diagnostic based on the Gelman and Rubin statistics. As the original code, this version implements an efficient sampling of the posterior distribution using the fast/slow parameter decorrelations [54], and it includes the support for the Planck data release 2015 Likelihood Code [47] (see http://cosmologist.info/cosmomc/).

IV. RESULTS

The constraints at 68% C.L. on the cosmological parameters obtained by including the interaction between dark matter and dark energy are given in Tables I and II for the "Planck TT + lowTEB" and the "Planck TTTEEE+ lowTEB" baseline data sets, respectively. Those obtained allowing also for a freely-varying dark energy equation of state are shown in Tables III and IV. For comparison purposes we also quote in Table V the bounds on the cosmological parameters as obtained from the Planck collaboration [1] in the pure ΛCDM and wCDM context, i.e., without considering the dark matter-dark energy coupling ξ.

Notice, first of all, that the CMB-only constraints on the coupling ξ are very similar with or without the inclusion of the polarization data from Planck at higher multipoles. Tables I and II show that, in the $\Lambda\mathrm{CDM} + \xi$ scenario, CMB data only imposes a lower limit in the coupling $\xi > -0.23$ at 68% C.L., with or without the Planck small-scale polarization data.

However, if we compare the CMB constraints on the Hubble constant in Tables I and II in the presence of a coupling ξ to those obtained with no interaction in Table V, we see that the coupling produces a shift at more than 2σ towards higher values of the Hubble constant and relaxes the error bars by a factor ~ 2. The fact that interacting dark energy alleviates the H_0 tension can also be noticed in the results depicted by the confidence level contours in the (ξ, H_0) planes in Fig. 1. The reason for that is the following: within the interacting dark matter-dark energy model explored here, the dark matter density contribution is required to be smaller, as for negative ξ the dark matter density will get an extra contribution proportional to the

TABLE I. 68% C.L. constraints on cosmological parameters from the "Planck TT + lowTEB" baseline dataset and its further combinations with several datasets (see text). An interacting dark energy model with negative coupling $\xi \leq 0$ is assumed. Please note that in case of the "tau055" prior the "lowTEB" dataset is not considered.

Parameter	Planck TT +lowTEB	Planck TT +lowTEB + R16	Planck TT +lowTEB + BAO	Planck TT +lowTEB + JLA	Planck TT +lowTEB + WL	Planck TT +lowTEB + lensing	Planck TT +tau055	Planck TT + lowTEB +JLA + BAO + R16
$\Omega_b h^2$	0.02222 ± 0.00023	0.02235 ± 0.00022	0.02221 ± 0.00020	0.02220 ± 0.00023	0.02232 ± 0.00023	0.02225 ± 0.00023	0.02207 ± 0.00021	0.02227 ± 0.00021
$\Omega_c h^2$	$0.100^{+0.017}_{-0.011}$	$0.088^{+0.006}_{-0.013}$	$0.104^{+0.015}_{-0.007}$	$0.104^{+0.014}_{-0.007}$	$0.098^{+0.016}_{-0.011}$	$0.099^{+0.017}_{-0.011}$	$0.098^{+0.012}_{-0.018}$	$0.100^{+0.012}_{-0.010}$
τ	0.076 ± 0.019	0.082 ± 0.019	0.076 ± 0.0018	0.076 ± 0.019	0.075 ± 0.019	0.065 ± 0.016	0.0587 ± 0.0089	0.079 ± 0.018
n_s	0.9652 ± 0.0061	0.9696 ± 0.0059	0.9650 ± 0.0047	0.9648 ± 0.0059	0.9691 ± 0.0060	0.9675 ± 0.0059	0.9585 ± 0.0058	0.9664 ± 0.0047
$\ln(10^{10} A_s)$	3.087 ± 0.036	3.095 ± 0.037	3.087 ± 0.035	3.087 ± 0.036	3.080 ± 0.037	3.061 ± 0.029	3.057 ± 0.018	3.091 ± 0.035
H_0 [km s^{-1} Mpc^{-1}]	69.0 ± 1.4	$70.7^{+1.2}_{-1.0}$	$68.63^{+0.8}_{-1.0}$	68.6 ± 1.2	69.8 ± 1.4	69.5 ± 1.4	$68.4^{+1.6}_{-1.4}$	69.22 ± 0.77
σ_8	$1.01^{+0.08}_{-0.19}$	$1.13^{+0.18}_{-0.10}$	$0.967^{+0.05}_{-0.15}$	$0.964^{+0.05}_{-0.14}$	$1.01^{+0.09}_{-0.19}$	$1.00^{+0.09}_{-0.19}$	$1.04^{+0.12}_{-0.22}$	$1.01^{+0.08}_{-0.16}$
Ω_m	0.260 ± 0.036	$0.223^{+0.015}_{-0.032}$	$0.270^{+0.038}_{-0.021}$	$0.272^{+0.036}_{-0.025}$	0.249 ± 0.033	0.252 ± 0.035	$0.260^{+0.033}_{-0.051}$	0.256 ± 0.026
ξ	> -0.232	$-0.25^{+0.05}_{-0.10}$	> -0.184	> -0.181	$-0.17^{+0.12}_{-0.10}$	> -0.232	$-0.21^{+0.09}_{-0.16}$	$-0.18^{+0.11}_{-0.10}$
$\lvert \log B_{01} \rvert$ (SDDR)	0	1.52	0	0.04	0.11	0.01	0.23	0.39

TABLE II. 68% C.L. constraints on cosmological parameters from the "Planck TTTEEE + lowTEB" baseline dataset and its further combinations with several datasets (see text). An interacting dark energy model with negative coupling $\xi \leq 0$ is assumed. Please note that in case of the "tau055" prior the "lowTEB" dataset is not considered.

Parameter	Planck TTTEEE +lowTEB	Planck TTTEEE +lowTEB + R16	Planck TTTEEE +lowTEB + BAO	Planck TTTEEE +lowTEB + JLA	Planck TTTEEE +lowTEB + WL	Planck TTTEEE +lowTEB + lensing	Planck TTTEEE +tau055	Planck TTTEEE +lowTEB + JLA +BAO + R16
$\Omega_b h^2$	0.02223 ± 0.00016	0.02230 ± 0.00015	0.02223 ± 0.00014	0.02222 ± 0.00015	0.02228 ± 0.00016	0.02224 ± 0.00016	0.02214 ± 0.00015	0.02226 ± 0.00014
$\Omega_c h^2$	$0.101^{+0.017}_{-0.010}$	$0.089^{+0.005}_{-0.012}$	$0.104^{+0.014}_{-0.007}$	$0.104^{+0.014}_{-0.007}$	$0.099^{+0.017}_{-0.011}$	$0.097^{+0.018}_{-0.010}$	$0.097^{+0.011}_{-0.018}$	$0.099^{+0.012}_{-0.010}$
τ	0.077 ± 0.017	0.081 ± 0.017	0.078 ± 0.0016	0.078 ± 0.017	0.074 ± 0.017	0.062 ± 0.014	0.0602 ± 0.0087	0.080 ± 0.017
n_s	0.9641 ± 0.0047	0.9664 ± 0.0048	0.9643 ± 0.0043	0.9641 ± 0.0047	0.9660 ± 0.0048	0.9652 ± 0.0047	0.9593 ± 0.0046	0.9651 ± 0.0043
$\ln(10^{10} A_s)$	3.090 ± 0.033	3.095 ± 0.033	3.091 ± 0.032	3.091 ± 0.033	3.082 ± 0.033	3.056 ± 0.025	3.059 ± 0.018	3.094 ± 0.033
H_0 [km s^{-1} Mpc^{-1}]	68.9 ± 1.2	$70.2^{+1.1}_{-0.8}$	$68.58^{+0.8}_{-1.1}$	$68.57^{+0.9}_{-1.2}$	69.3 ± 1.2	69.2 ± 1.2	$68.7^{+1.4}_{-1.3}$	69.20 ± 0.78
σ_8	$1.01^{+0.08}_{-0.19}$	$1.14^{+0.017}_{-0.09}$	$0.966^{+0.05}_{-0.15}$	$0.967^{+0.05}_{-0.14}$	$1.01^{+0.09}_{-0.19}$	$0.99^{+0.08}_{-0.19}$	$1.05^{+0.12}_{-0.21}$	$1.02^{+0.08}_{-0.16}$
Ω_m	$0.261^{+0.044}_{-0.035}$	$0.227^{+0.014}_{-0.031}$	$0.271^{+0.039}_{-0.021}$	$0.271^{+0.038}_{-0.023}$	$0.254^{+0.041}_{-0.036}$	$0.257^{+0.044}_{-0.034}$	$0.255^{+0.030}_{-0.049}$	0.254 ± 0.026
ξ	> -0.229	$-0.259^{+0.043}_{-0.098}$	> -0.182	> -0.182	$-0.18^{+0.13}_{-0.10}$	> -0.230	$-0.21^{+0.08}_{-0.15}$	-0.19 ± 0.089
$\lvert \log B_{01} \rvert$ (SDDR)	0.04	1.80	0	0.08	0.09	0	0.31	0.53

TABLE III. 68% C.L. constraints on cosmological parameters from the "Planck TT + lowTEB" baseline dataset and its further combinations with several datasets (see text). An interacting dark energy model with negative coupling $\xi \leq 0$ and a dark energy equation of state w are assumed. Please note that in case of the "tau055" prior the "lowTEB" dataset is not considered.

Parameter	Planck TT +lowTEB	Planck TT +lowTEB + R16	Planck TT +lowTEB + BAO	Planck TT +lowTEB + JLA	Planck TT +lowTEB + WL	Planck TT +lowTEB + lensing	Planck TT +tau055	Planck TT +lowTEB + JLA +BAO + R16
$\Omega_b h^2$	0.02226 ± 0.00023	0.02222 ± 0.00023	0.02228 ± 0.0022	0.02223 ± 0.00023	0.02235 ± 0.00023	0.02228 ± 0.00023	0.02211 ± 0.00022	0.02228 ± 0.00021
$\Omega_c h^2$	$0.100^{+0.016}_{-0.010}$	$0.101^{+0.015}_{-0.010}$	$0.088^{+0.012}_{-0.022}$	$0.089^{+0.012}_{-0.022}$	$0.101^{+0.014}_{-0.008}$	$0.097^{+0.017}_{-0.010}$	$0.099^{+0.020}_{-0.010}$	$0.089^{+0.027}_{-0.022}$
τ	0.074 ± 0.020	0.074 ± 0.020	0.079 ± 0.0019	0.076 ± 0.020	0.073 ± 0.020	0.060 ± 0.018	0.0580 ± 0.0087	0.078 ± 0.019
n_s	0.9657 ± 0.0062	0.9647 ± 0.0061	0.9672 ± 0.0056	0.9656 ± 0.0062	0.9692 ± 0.0060	0.9682 ± 0.0061	0.9589 ± 0.0059	0.9664 ± 0.0052
$\ln(10^{10}A_s)$	3.082 ± 0.038	3.083 ± 0.037	3.091 ± 0.037	3.086 ± 0.038	3.076 ± 0.038	3.050 ± 0.033	3.055 ± 0.018	3.089 ± 0.036
H_0 [km s^{-1} Mpc^{-1}]	82^{+10}_{-8}	$74.3^{+2.1}_{-1.7}$	$67.7^{+1.3}_{-1.6}$	67.9 ± 1.5	86^{+10}_{-5}	79 ± 10	78^{+10}_{-20}	$69.13^{+0.9}_{-1.0}$
σ_8	$1.12^{+0.17}_{-0.09}$	$1.05^{+0.08}_{-0.15}$	1.08 ± 0.15	1.09 ± 0.15	$1.12^{+0.14}_{-0.10}$	$1.09^{+0.18}_{-0.12}$	$1.11^{+0.18}_{-0.10}$	1.10 ± 0.15
Ω_m	$0.190^{+0.022}_{-0.059}$	0.224 ± 0.025	$0.243^{+0.027}_{-0.049}$	$0.242^{+0.029}_{-0.048}$	$0.174^{+0.017}_{-0.047}$	$0.199^{+0.28}_{-0.70}$	$0.212^{+0.032}_{-0.076}$	0.234 ± 0.033
ξ	> -0.194	$-0.17^{+0.13}_{-0.08}$	$-0.26^{+0.09}_{-0.18}$	$-0.27^{+0.09}_{-0.18}$	$-0.13^{+0.12}_{-0.04}$	$-0.17^{+0.16}_{-0.05}$	> -0.241	> -0.346
w	$-1.39^{+0.24}_{-0.41}$	$-1.178^{+0.063}_{-0.070}$	$-0.918^{+0.076}_{-0.062}$	-0.932 ± 0.067	$-1.48^{+0.20}_{-0.33}$	-1.29 ± 0.33	-1.29 ± 0.38	$-0.969^{+0.074}_{-0.034}$
$\lvert \log B_{01} \rvert$ (SDDR)	0.08	0.18	0.28	0.34	0.10	0.15	0.12	0.23

TABLE IV. 68% C.L. constraints on cosmological parameters from the "Planck TTTEEE + lowTEB" baseline dataset and its further combinations with several datasets (see text). An interacting dark energy model with negative coupling $\xi \leq 0$ and a dark energy equation of state w are assumed. Please note that in case of the "tau055" prior the "lowTEB" dataset is not considered.

Parameter	Planck TTTEEE +lowTEB	Planck TTTEEE +lowTEB + $R16$	Planck TTTEEE +lowTEB + BAO	Planck TTTEEE +lowTEB + JLA	Planck TTTEEE +lowTEB + WL	Planck TTTEEE +lowTEB + lensing	Planck TTTEEE +tau055	Planck TTTEEE +lowTEB + JLA +BAO + $R16$
$\Omega_b h^2$	0.02225 ± 0.00016	0.02223 ± 0.00016	0.02226 ± 0.00015	0.02224 ± 0.00016	0.02231 ± 0.00016	0.02224 ± 0.00016	0.02218 ± 0.00015	0.02228 ± 0.00015
$\Omega_c h^2$	$0.100^{+0.016}_{-0.009}$	$0.101^{+0.014}_{-0.010}$	$0.090^{+0.012}_{-0.022}$	$0.089^{+0.011}_{-0.022}$	$0.102^{+0.013}_{-0.008}$	$0.097^{+0.018}_{-0.011}$	$0.099^{+0.019}_{-0.010}$	$0.089^{+0.028}_{-0.022}$
τ	0.074 ± 0.017	0.075 ± 0.017	0.079 ± 0.017	0.078 ± 0.017	0.070 ± 0.017	0.054 ± 0.015	0.0597 ± 0.0089	0.079 ± 0.016
n_s	0.9644 ± 0.0048	0.9636 ± 0.0045	0.9652 ± 0.0046	0.9644 ± 0.0049	0.9660 ± 0.0047	0.9650 ± 0.0048	0.9601 ± 0.0046	0.9651 ± 0.0045
$\ln(10^{10}A_s)$	3.082 ± 0.033	3.085 ± 0.033	3.092 ± 0.033	3.091 ± 0.033	3.072 ± 0.033	$3.040^{+0.027}_{-0.031}$	3.058 ± 0.018	3.092 ± 0.032
H_0[km s^{-1} Mpc^{-1}]	82^{+10}_{-8}	$74.4^{+2.0}_{-1.7}$	$68.0^{+1.3}_{-1.5}$	67.9 ± 1.4	86^{+10}_{-6}	79^{+10}_{-20}	79 ± 10	69.14 ± 0.91
σ_8	$1.13^{+0.16}_{-0.09}$	$1.05^{+0.08}_{-0.14}$	$1.08^{+0.14}_{-0.20}$	1.09 ± 0.15	$1.13^{+0.15}_{-0.09}$	$1.09^{+0.18}_{-0.11}$	$1.11^{+0.17}_{-0.11}$	1.10 ± 0.15
Ω_m	$0.188^{+0.023}_{-0.055}$	0.225 ± 0.026	$0.244^{+0.027}_{-0.048}$	$0.244^{+0.026}_{-0.049}$	$0.173^{+0.017}_{-0.045}$	$0.201^{+0.029}_{-0.069}$	$0.203^{+0.029}_{-0.067}$	0.234 ± 0.033
ξ	$-0.16^{+0.14}_{-0.06}$	$-0.16^{+0.11}_{-0.09}$	$-0.26^{+0.09}_{-0.18}$	> -0.351	$-0.13^{+0.11}_{-0.05}$	$-0.19^{+0.17}_{-0.06}$	> -0.222	> -0.351
w	$-1.41^{+0.24}_{-0.40}$	-1.185 ± 0.064	$-0.935^{+0.069}_{-0.054}$	-0.934 ± 0.064	$-1.52^{+0.20}_{-0.32}$	-1.28 ± 0.35	-1.33 ± 0.35	$-0.973^{+0.067}_{-0.032}$
$\lvert \log B_{01} \rvert$ (SDDR)	0.22	0.13	0.29	0.25	0.14	0.13	0.09	0.23

TABLE V. 68% C.L. constraints on cosmological parameters from the “Planck TTTEEE + lowTEB” baseline dataset and its combination with external datasets assuming ΛCDM and wCDM models in the absence of an interaction, i.e. $\xi = 0$.

Parameter	Planck TTTEEE +lowTEB	Planck TTTEEE +lowTEB + BAO	Planck TTTEEE +lowTEB + JLA	Planck TTTEEE +lowTEB + lensing	Planck TTTEEE +lowTEB	Planck TTTEEE +lowTEB + BAO	Planck TTTEEE +lowTEB + JLA	Planck TTTEEE +lowTEB + lensing
$\Omega_b h^2$	0.02226 ± 0.00015	0.02229 ± 0.00014	0.02227 ± 0.00015	0.02226 ± 0.00016	0.02228 ± 0.00016	0.02227 ± 0.00015	0.02225 ± 0.00016	0.02228 ± 0.00016
$\Omega_c h^2$	0.1198 ± 0.0014	0.1193 ± 0.0011	0.1196 ± 0.0014	0.1193 ± 0.0014	0.1196 ± 0.0015	0.1196 ± 0.0014	0.1198 ± 0.0015	0.1191 ± 0.0014
τ	0.079 ± 0.017	0.082 ± 0.016	0.080 ± 0.017	0.062 ± 0.014	0.076 ± 0.017	0.080 ± 0.017	0.079 ± 0.017	0.056 ± 0.015
n_s	0.9646 ± 0.0047	0.9661 ± 0.0041	0.9650 ± 0.0047	0.9652 ± 0.0048	0.9649 ± 0.0047	0.9651 ± 0.0046	0.9645 ± 0.0047	0.9657 ± 0.0047
$\ln(10^{10}A_s)$	3.094 ± 0.034	3.098 ± 0.032	3.094 ± 0.033	3.058 ± 0.025	3.086 ± 0.034	3.095 ± 0.034	3.093 ± 0.033	3.044 ± 0.028
$H_0[\mathrm{km\,s^{-1}\,Mpc^{-1}}]$	67.30 ± 0.64	67.53 ± 0.48	67.36 ± 0.64	67.50 ± 0.64	> 80.9	$68.2^{+1.4}_{-1.7}$	68.3 ± 1.6	> 75.3
σ_8	$0.831^{+0.015}_{-0.013}$	0.832 ± 0.013	0.831 ± 0.013	0.8146 ± 0.0088	$0.98^{+0.11}_{-0.06}$	0.839 ± 0.022	0.841 ± 0.020	$0.924^{+0.12}_{-0.07}$
Ω_m	0.3152 ± 0.0089	0.3119 ± 0.0065	0.3142 ± 0.0089	$0.3122^{+0.0084}_{-0.0095}$	$0.205^{+0.023}_{-0.066}$	0.307 ± 0.013	$0.307^{+0.014}_{-0.017}$	$0.227^{+0.036}_{-0.089}$
w	$[-1]$	$[-1]$	$[-1]$	$[-1]$	$-1.54^{+0.19}_{-0.38}$	$-1.030^{+0.070}_{-0.058}$	-1.034 ± 0.053	$-1.42^{+0.27}_{-0.45}$

dark energy one. Since CMB accurately constrains $\Omega_c h^2$, a larger value of H_0 will be required in these scenarios, which in turn, will provide a better agreement with the direct measurement of H_0 from the R16 prior. More quantitatively, notice, from the first column of Table II, that we obtain $H_0 = 68.9 \pm 1.2$ km/s/Mpc for “Planck TTTEEE+ lowTEB” while, without interaction and for the same combination of datasets, we have $H_0 = 67.30 \pm 0.64$ km/s/Mpc as can be noticed from the first column of Table V. This effect reduces at 2σ the tension of the Planck CMB anisotropy data in a ΛCDM framework with Riess *et al.* 2016 [3] (i.e. with the value $H_0 = 73.24 \pm 1.74$ km/s/Mpc. It should not therefore come as a surprise that when the R16 prior on the Hubble constant is added in the analyses, a preference for a nonzero coupling appears with a significance larger than 2 standard deviations (see also Fig. 1). Indeed, the “Planck TT + lowTEB + R16” data set (see Table I) gives $\xi = -0.25^{+0.05}_{-0.10}$ at 68% C.L. ($\xi = -0.25^{+0.17}_{-0.13}$ at 95% C.L.), while the “Planck TTTEEE+ lowTEB + R16” data set (see Tab. II) gives $\xi = -0.259^{+0.043}_{-0.098}$ at 68% C.L. ($\xi = -0.26^{+0.16}_{-0.12}$ at 95% C.L.). However, when we add other data sets to this combination, we find that “Planck TT + lowTEB + R16 + JLA + BAO” (see Table I) gives $\xi = -0.18^{+0.11}_{-0.10}$ at 68% C.L. ($\xi > -0.330$ at 95% C.L.) and “Planck TTTEEE + lowTEB + R16+ JLA + BAO” (see Table II) gives $\xi = -0.19 \pm 0.089$ at 68% C.L. ($\xi = -0.19^{+0.16}_{-0.17}$ at 95% C.L.), reducing the significance for a nonzero coupling.

While the Planck + R16 combined data sets clearly show evidence for a coupling, also other data sets seem to suggest this possibility. When the WL data set is included a hint (slightly above one standard deviation) is indeed present. The “Planck TT + lowTEB + WL” data set (see Table I) gives $\xi = -0.17^{+0.12}_{-0.10}$ at 68% C.L., while the “Planck TTTEEE+ lowTEB + WL” data set (see Table II) gives $\xi = -0.18^{+0.13}_{-0.10}$ at 68% C.L. It is worthwhile to note that when the interacting dark energy is introduced, a very large shift towards lower values of the cold dark matter density $\Omega_c h^2$ appears and the error bars are relaxed by a factor 10, as can be seen by comparing the results of Tables I and II with those shown in Table V. Moreover, we find a shift of the clustering parameter σ_8 towards an higher value, compensated by a lowering of the matter density Ω_m, both with relaxed error bars. In this way, we are not increasing the tension on the S_8 parameter between Planck CMB data and the weak lensing measurements from the CFHTLenS survey [4,5] and KiDS-450 [6]. This can be also clearly noticed from the left panel of Fig. 2, where we plot the two-dimensional constraints on the Ω_m-σ_8 plane from the “Planck TTTEEE + lowTEB” data set in the cases of $\xi = 0$, nonzero coupling, and combined with the WL measurements.

Also when the “tau055” prior is included a small preference for a nonzero dark matter-dark energy coupling seems to emerge. The reported constraints of

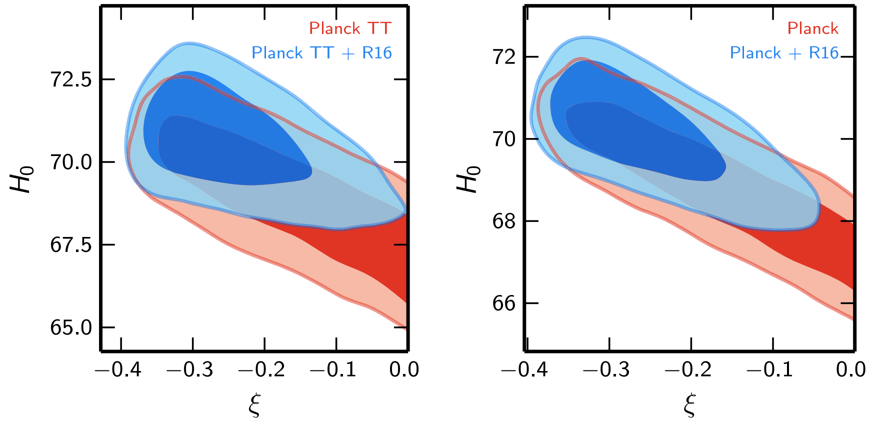

FIG. 1. 68% and 95% C.L. in the two-dimensional (ξ, H_0) planes from the "Planck TT + lowTEB" dataset (left panel) and "Planck TTTEEE + lowTEB" dataset (right panel) also combined with the R16 prior on the Hubble constant. Notice that the presence of a coupling ξ allows for larger values for H_0 from Planck data. The inclusion of the R16 prior results in an indication for $\xi < 0$ with a significance above two standard deviations.

$\xi = -0.21^{+0.09}_{-0.16}$ at 68% C.L. for the "Planck TT + tau055" and $\xi = -0.21^{+0.08}_{-0.15}$ at 68% C.L. for the "Planck TTTEEE+ tau055" data sets respectively could naively suggest a statistically significant detection (at more than 2 standard deviations) for a dark energy-dark matter interaction. It is however important to point out that the posterior distribution for ξ is in this case highly non-Gaussian. At 95% C.L. we have found that the tau055 prior gives no indication for an interaction, providing a lower limit only. We obtain $\xi > -0.37$ for the "Planck TT + tau055" data set, and $\xi > -0.38$ for the "Planck TTTEEE + tau055" data set, respectively, both at 95% C.L. Therefore, while the tau055 prior suggests a value of $\xi < 0$, this indication is not statistically significant (only slightly above 1σ); notice this fact from the right panel of Fig. 2, where we plot the two-dimensional posteriors in the ξ vs τ plane. This preference is driven by the smaller value required in interacting dark energy models for the present dark matter mass-energy density, which would itself lead to a lower value of τ.

In a second step, we consider the dark energy equation of state w free to vary. Indeed, if dark energy is an interacting fluid, it is expected that its equation of state differs from the canonical value in the ΛCDM scenario, $w = -1$. As we can see from the values reported in Tables III and IV and from Fig. 3, where we plot the two-dimensional posteriors in the H_0 vs w plane, the inclusion of a negative coupling ξ makes models with larger values of w in better agreement with the CMB data. Indeed, from the "Planck TTTEEE + lowTEB" data set, we obtain the upper limit $w < -1.17$ at 68% C.L. when a negative coupling is considered (see Table IV), to be compared with the limit $w < -1.35$ at 68% C.L. obtained when we fix $\xi = 0$ (see Table V). This fact results

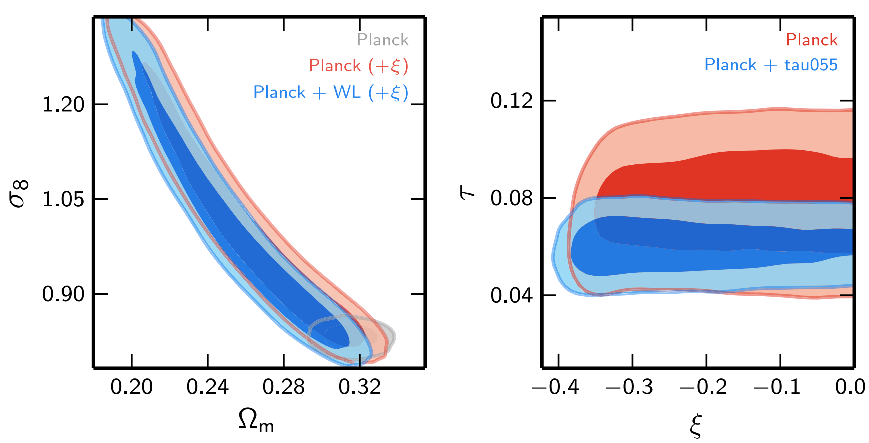

FIG. 2. Left panel: 68% and 95% C.L. in the two-dimensional (Ω_m, σ_8) plane from the "Planck TTTEEE + lowTEB" dataset for a pure ΛCDM scenario, a varying ξ interacting model, and also adding to the former the WL data set. Notice that the coupling allows for larger values for σ_8 and smaller values for Ω_m, relaxing the Planck bounds on the S_8 parameter and mildly alleviating the tension with the S_8 values measured by cosmic shear surveys as CFHTLenS and KiDS-450. Right panel: 68% and 95% C.L. in the two-dimensional (ξ, τ) plane from the "Planck TTTEEE " data set, and also combined with the "tau055" prior on the reionization optical depth. Notice that the "tau055" prior affects only marginally the constraints on ξ, resulting in a $\sim 1\sigma$ indication for $\xi < 0$ (after marginalization over τ).

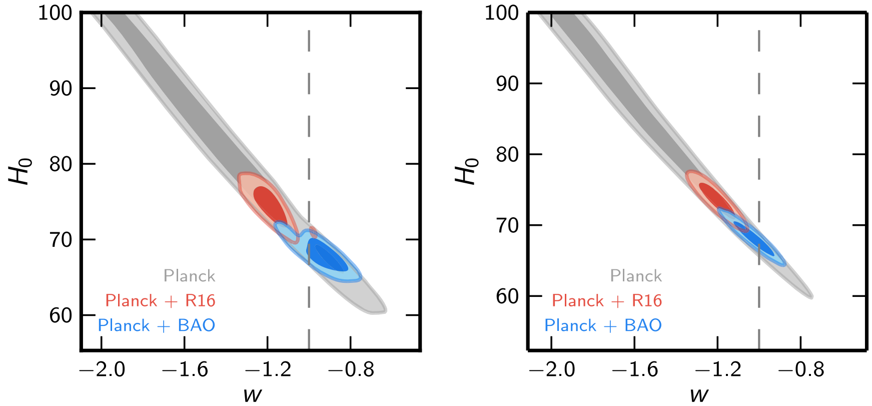

FIG. 3. Left panel: 68% and 95% C.L. in the two-dimensional (w, H_0) plane from the combination of "Planck TTTEEE + lowTEB" measurements (grey contours), "Planck TTTEEE + lowTEB + R16" (red contours) and "Planck TTTEEE + lowTEB + BAO" (blue contours), for an interacting dark matter-dark energy scenario. Right panel: As in the left panel but with $\xi = 0$.

even more evident by the comparison of the two-dimensional posteriors in the H_0 vs w plane depicted in Fig. 3 from the "Planck TTTEEE + lowTEB" data set in the case of a negative coupling (left panel) to those with $\xi = 0$ (right panel). The CMB-only contours clearly extend to larger values of w in the presence of a negative coupling. Furthermore, the posterior in this case appears as bimodal: there is a significant portion of models with $w > -1$ and $\xi < 0$ compatible with the data. The reason for this is simple: models with negative coupling mimic an effective equation of state with $w < -1$. Increasing w has therefore a similar effect of decreasing ξ and this enhances the compatibility of models with $w > -1$ with the data. Also from Fig. 3 (and as it is well known), one can clearly noticed that when a variation in w is considered, the Planck constraints on the Hubble constant practically vanish. In this case we can safely include the R16 prior on the Hubble constant, as the tension between Planck and R16 disappears, finding for this particular combination a detection of $w < -1$ at more than 2σ, obtaining $w = -1.178^{+0.063}_{-0.070}$ from "Planck TT + lowTEB + R16" (see Table III) and $w = -1.185 \pm 0.064$ from "Planck TTTEEE + lowTEB+ R16" (see Table IV), both at 68% C.L.

When a variation on w is included, the previous hint for $\xi < 0$ from the Planck + R16 data set is still present but relaxed. In fact, there is still an hint at about 1σ for $\xi < 0$ from the "Planck TT + R16" data set that persists when the Planck polarization data is included: we obtain $\xi = -0.17^{+0.13}_{-0.08}$ from "Planck TT + lowTEB + R16" (see Table III) and $\xi = -0.16^{+0.11}_{-0.09}$ from "Planck TTTEEE+ lowTEB + R16" (see Table IV), both at 68% C.L. As we can see from Fig. 3 the contour plots in the case of "Planck TTTEEE + lowTEB + R16" (left panel) fully confirm the preference for $w < -1$ but also appear as slightly bimodal. The reason is that, for stability reasons, we have not considered models with positive coupling ξ that would have been degenerate with models with $w < -1$. Once again, introducing models with negative coupling increases the compatibility with the data of models in which $w > -1$, however in case of the R16 prior this is not enough to prevent an indication for $w < -1$ at more than 95% C.L. It is important to note that this preference for $\xi < 0$ disappears completely when considering the combination "Planck TT + lowTEB + R16 + JLA + BAO" or "Planck TTTEEE + lowTEB + R16 + JLA + BAO", as we can see in the Tables III and IV, and w is in agreement with -1 within 1 standard deviation.

In fact, when either BAO or JLA measurements are added separately in the analyses the indication for $w < -1$ disappears and a cosmological constant is now consistent with the data within two standard deviations. It is interesting to note, from Table III, that in the case of "Planck TT + lowTEB + BAO" and "Planck TTTEEE + lowTEB + BAO" data sets one gets the constraint $\xi = -0.26^{+0.09}_{-0.18}$ at 68% C.L., apparently suggesting a dark matter-dark energy coupling at more than 2σ. This is probably due to the small tension present between the Planck and BAO data. We have found however that also in this case the posterior for ξ is highly non-Gaussian and that the indication for a coupling from this data set is only slightly larger than one standard deviation. Indeed, if we consider the two standard deviation constraint we obtain only a lower limit ($\xi > -0.427$ at 95% C.L.). Since a negative coupling is degenerate with models in which $w > -1$, we find that, when the BAO or JLA data sets are included, the constraints on w are shifted towards larger values with respect to the case with no coupling, hinting to $w > -1$ at more than one standard deviation. Indeed, we get $w = -0.918^{+0.076}_{-0.062}$ from "Planck TT + lowTEB+ BAO" (see Table III) and $w = -0.935^{+0.069}_{-0.054}$ from "Planck TTTEEE + lowTEB + BAO" (see Table IV), both at 68% C.L. to be compared to the value $w = -1.030^{+0.070}_{-0.058}$ from "Planck TTTEEE + lowTEB + BAO" at 68% C.L. but with no coupling (see Table V). Similarly, we get

$w = -0.932 \pm -0.067$ from "Planck TT + lowTEB+ JLA" (see Table III) and $w = -0.934 \pm 0.064$ from "Planck TTTEEE + lowTEB + JLA" (see Table IV) at 68% C.L., to be compared to the value $w = -1.034 \pm 0.053$ obtained from "Planck TTTEEE + lowTEB + JLA" at 68% C.L. but with $\xi = 0$ (see Table V).

Within the wCDM + ξ scenario, the shift towards lower values of the cold dark matter density $\Omega_c h^2$ is incremented, as can be noticed by comparing the results in Table IV with those in Table V, and therefore the tension between the Planck values and the weak lensing estimations of the S_8 parameter gets alleviated. When the WL data set is included one gets an indication for a negative coupling and $w < -1$ at slightly more than one standard deviation.

V. BAYESIAN EVIDENCE WITH THE SAVAGE–DICKEY DENSITY RATIO

Given the indication for $\xi < 0$ from the analysis presented in the previous section it is certainly useful to better quantify the Bayesian evidence for an interacting dark energy model from all the considered data sets. In what follows we make use of the Savage-Dickey density ratio (SDDR), that is helpful in reducing the computational effort needed to calculate the Bayes factor of two nested models (see e.g. [55–57]). Assuming SDDRD the Bayes factor B_{01} can be written as

$$B_{01} = \left.\frac{p(\xi|d, M_1)}{\pi(\xi|M_1)}\right|_{\xi=0} (\mathrm{SDDR}), \tag{10}$$

where M_1 is the interacting dark energy model, $p(\xi|d, M_1)$ is the posterior for ξ in this theoretical framework computed from a specific data set d, and $\pi(\xi|M_1)$ is the prior on ξ that we assume as flat in the range $-1 \leq \xi \leq 0$.

It is usual to consider the logarithm of the Bayes factor, for which the so–called "Jeffreys' scale" gives empirically calibrated levels of significance for the strength of evidence: $|\ln B_{01}| < 1.0$ is inconclusive, $|\ln B_{01}| = 1.0$ gives a positive evidence, $|\ln B_{01}| = 2.5$ provides a moderate evidence and, finally, $|\ln B_{01}| = 5.0$ means a strong evidence.

At the bottom of Tables I, II, III, and IV we report the Bayesian evidence for each data set considered.

As we can see, when assuming a dark energy component with $w = -1$ (Tables I and II) we identify a Positive evidence (> 1) for $\xi < 0$ from the combined Planck TT + lowTEB + R16 and Planck TTTEEE + lowTEB + R16 data sets. Again, interacting dark energy helps in solving the H_0 tension, while for all the other data sets the evidence is inconclusive.

However, when we consider also variations in w (see Tables III and IV) also the evidence in the case of the Planck TT + lowTEB + R16 and Planck TTTEEE + lowTEB + R16 data sets is inconclusive, i.e. we do not need interacting dark energy to solve the H_0 tension since this is solved by having $w < -1$.

VI. CONCLUSIONS

We have explored the well-known Hubble constant H_0 tension between the current estimates from late-time universe data of Riess *et al.* 2016, which indicates a value of $H_0 = 73.24 \pm 1.74$ km/s/Mpc and the Planck cosmic microwave background (CMB) measurement of $H_0 = 66.93 \pm 0.62$ km/s/Mpc (both at 68% C.L.), in the context of interacting dark matter-dark energy scenarios. Such a coupling could affect the value of the present matter energy density Ω_m. Therefore, if within an interacting model Ω_m is smaller, a larger value of H_0 would be required in order to satisfy the peaks structure of CMB observations, which accurately determine the value of $\Omega_m h^2$. We find that for one of the most interesting and viable coupled dark matter-dark energy scenarios in the literature, in which the exchanged energy rate is negative (i.e. the energy flows from the dark matter system to the dark energy one) and proportional to the dark energy density, the existing $3\sigma H_0$ tension is alleviated. In addition, when combining CMB measurements with the Hubble constant prior from Riess *et al.* 2016, a preference for a nonzero coupling appears with a significance larger than 2σ. Computing the Bayesian evidence using the SDDR for this case, we have found a marginal positive evidence ($|\ln B_{01}| = 1.8$) for interacting dark energy, i.e. with an odds ratio of 6:1 respect to a cosmological constant. The Bayesian evidence for interacting dark energy is inconclusive for all other data sets combination. However, it is certainly not unexpected that in interacting scenarios the dark energy equation of state differs from its canonical value within the ΛCDM picture, i.e., is different from $w = -1$. We have therefore considered as well such a possibility, finding that, when the dark energy equation of state w is also a free parameter, the Hubble constant tension gets strongly alleviated, obtaining $\sim 3\sigma$ indication for a phantomlike ($w < -1$) dark energy fluid when combining CMB and Riess *et al.* 2016 measurements. In this case there is However, when other data sets, as BAO or Supernovae Ia luminosity distances from JLA, are also included in our numerical analyses, a good consistency with a pure ΛCDM cosmological scenario is found with models with negative coupling and $w > -1$ suggested at slightly more than one standard deviation.

ACKNOWLEDGMENTS

We would like to thank Laura Lopez-Honorez for stimulating discussions and help with the numerical codes. We thank the anonymous referee for suggesting us the use of SDDR for computing the Bayesian evidence. The work done by A. M. is also supported by TASP/INFN. O. M. is supported by PROMETEO II/2014/050, by the Spanish

Grant No. FPA2014–57816-P of the MINECO, by the MINECO Grant No. SEV-2014-0398 and by the European Union's Horizon 2020 research and innovation programme under the Marie Sklodowska-Curie grant agreements 690575 and 674896. This work has been done within the Labex ILP (reference ANR-10-LABX-63) part of the Idex SUPER, and received financial state aid managed by the Agence Nationale de la Recherche, as part of the programme Investissements d'avenir under the reference ANR-11-IDEX-0004-02.

[1] P. A. R. Ade *et al.* (Planck Collaboration), Planck 2015 results. XIII. Cosmological parameters, Astron. Astrophys. **594**, A13 (2016).

[2] N. Aghanim *et al.* (Planck Collaboration), Planck intermediate results. XLVI. Reduction of large-scale systematic effects in HFI polarization maps and estimation of the reionization optical depth, Astron. Astrophys. **596**, A107 (2016).

[3] A. G. Riess *et al.*, A 2.4% determination of the local value of the Hubble constant, Astrophys. J. **826**, 56 (2016).

[4] C. Heymans *et al.*, CFHTLenS: The Canada-France-Hawaii Telescope Lensing Survey, Mon. Not. R. Astron. Soc. **427**, 146 (2012).

[5] T. Erben *et al.*, CFHTLenS: The Canada-France-Hawaii Telescope Lensing Survey—Imaging data and catalogue products, Mon. Not. R. Astron. Soc. **433**, 2545 (2013).

[6] H. Hildebrandt *et al.*, KiDS-450: Cosmological parameter constraints from tomographic weak gravitational lensing, Mon. Not. R. Astron. Soc. **465**, 1454 (2017).

[7] S. Joudaki *et al.*, KiDS-450: Testing extensions to the standard cosmological model, arXiv:1610.04606.

[8] E. Di Valentino, A. Melchiorri, and J. Silk, Beyond six parameters: Extending ΛCDM, Phys. Rev. D **92**, 121302 (2015).

[9] E. Di Valentino, A. Melchiorri, and J. Silk, Reconciling Planck with the local value of H_0 in extended parameter space, Phys. Lett. B **761**, 242 (2016).

[10] J. L. Bernal, L. Verde, and A. G. Riess, The trouble with H_0, J. Cosmol. Astropart. Phys. 10 (2016) 019.

[11] R. J. Wilkinson, C. Boehm, and J. Lesgourgues, Constraining dark matter-neutrino interactions using the CMB and large-scale structure, J. Cosmol. Astropart. Phys. 05 (2014) 011.

[12] J. Lesgourgues, G. Marques-Tavares, and M. Schmaltz, Evidence for dark matter interactions in cosmological precision data?, J. Cosmol. Astropart. Phys. 02 (2016) 037.

[13] Z. Berezhiani, A. D. Dolgov, and I. I. Tkachev, Reconciling Planck results with low redshift astronomical measurements, Phys. Rev. D **92**, 061303 (2015).

[14] S. Gariazzo, M. Escudero, R. Diamanti, and O. Mena, Cosmological searches for a non-cold dark matter component, arXiv:1704.02991.

[15] S. Grandis, D. Rapetti, A. Saro, J. J. Mohr, and J. P. Dietrich, Quantifying tensions between CMB and distance datasets in models with free curvature or lensing amplitude, Mon. Not. R. Astron. Soc. **463**, 1416 (2016).

[16] M. M. Zhao, D. Z. He, J. F. Zhang, and X. Zhang, A search for sterile neutrinos in holographic dark energy cosmology: Reconciling Planck observation with the local measurement of Hubble constant, arXiv:1703.08456.

[17] W. Yang, R. C. Nunes, S. Pan, and D. F. Mota, Effects of neutrino mass hierarchies on dynamical dark energy models, Phys. Rev. D **95**, 103522 (2017).

[18] V. Prilepina and Y. Tsai, Reconciling large and small-scale structure in twin Higgs models, arXiv:1611.05879.

[19] E. Di Valentino and L. Mersini-Houghton, Testing predictions of the quantum landscape multiverse 2: The exponential inflationary potential, J. Cosmol. Astropart. Phys. 03 (2017) 020.

[20] B. Santos, A. A. Coley, N. C. Devi, and J. S. Alcaniz, Testing averaged cosmology with type Ia supernovae and BAO data, J. Cosmol. Astropart. Phys. 02 (2017) 047.

[21] S. Kumar and R. C. Nunes, Probing the interaction between dark matter and dark energy in the presence of massive neutrinos, Phys. Rev. D **94**, 123511 (2016).

[22] T. Karwal and M. Kamionkowski, Early dark energy, the Hubble-parameter tension, and the string axiverse, Phys. Rev. D **94**, 103523 (2016).

[23] P. Ko and Y. Tang, Light dark photon and fermionic dark radiation for the Hubble constant and the structure formation, Phys. Lett. B **762**, 462 (2016).

[24] M. Archidiacono, S. Gariazzo, C. Giunti, S. Hannestad, R. Hansen, M. Laveder, and T. Tram, Pseudoscalar—sterile neutrino interactions: reconciling the cosmos with neutrino oscillations, J. Cosmol. Astropart. Phys. 08 (2016) 067.

[25] Q. G. Huang and K. Wang, How the dark energy can reconcile Planck with local determination of the Hubble constant, Eur. Phys. J. C **76**, 506 (2016).

[26] Z. Chacko, Y. Cui, S. Hong, T. Okui, and Y. Tsai, Partially acoustic dark matter, interacting dark radiation, and large scale structure, J. High Energy Phys. 12 (2016) 108.

[27] Y. Zhang, H. Zhang, D. Wang, Y. Qi, Y. Wang, and G. B. Zhao, Probing dynamics of dark energy with latest observations, Res. Astron. Astrophys. **17**, 050 (2017).

[28] G. B. Zhao *et al.*, The clustering of galaxies in the completed SDSS-III Baryon Oscillation Spectroscopic Survey: Examining the observational evidence for dynamical dark energy, arXiv:1701.08165.

[29] J. Sola, J. d. C. Perez, and A. Gomez-Valent, Towards the firsts compelling signs of vacuum dynamics in modern cosmological observations, arXiv:1703.08218.

[30] C. Brust, Y. Cui, and K. Sigurdson, Cosmological constraints on interacting light particles, arXiv:1703.10732.

[31] L. Lancaster, F. Y. Cyr-Racine, L. Knox, and Z. Pan, A tale of two modes: Neutrino free-streaming in the early universe, arXiv:1704.06657.

[32] E. Di Valentino, A. Melchiorri, E. V. Linder, and J. Silk, Constraining dark energy dynamics in extended parameter space, arXiv:1704.00762.

[33] V. Salvatelli, N. Said, M. Bruni, A. Melchiorri, and D. Wands, Indications of a Late-Time Interaction in the Dark Sector, Phys. Rev. Lett. **113**, 181301 (2014).

[34] J. Sola, A. G. Valent, and J. C. Perez, Hints of dynamical vacuum energy in the expanding universe, Astrophys. J. Lett. **811**, L14 (2015).

[35] J. Sola, A. G. Valent, and J. C. Perez, First evidence of running cosmic vacuum: Challenging the concordance model, Astrophys. J. **836**, 43 (2017).

[36] C. Pigozzo, S. Carneiro, J. S. Alcaniz, H. A. Borges, and J. C. Fabris, Evidence for cosmological particle creation?, J. Cosmol. Astropart. Phys. 05 (2016) 022.

[37] M. G. Richarte and L. Xu, Exploring a new interaction between dark matter and dark energy using the growth rate of structure, arXiv:1506.02518.

[38] J. Väliviita and E. Palmgren, Distinguishing interacting dark energy from wCDM with CMB, lensing, and baryon acoustic oscillation data, J. Cosmol. Astropart. Phys. 07 (2015) 015.

[39] E. G. M. Ferreira, J. Quintin, A. A. Costa, E. Abdalla, and B. Wang, Evidence for interacting dark energy from BOSS, Phys. Rev. D **95**, 043520 (2017).

[40] R. Murgia, S. Gariazzo, and N. Fornengo, Constraints on the coupling between dark energy and dark matter from CMB data, J. Cosmol. Astropart. Phys. 04 (2016) 014.

[41] M. B. Gavela, D. Hernandez, L. Lopez Honorez, O. Mena, and S. Rigolin, Dark coupling, J. Cosmol. Astropart. Phys. 07 (2009) 034; Erratum, J. Cosmol. Astropart. Phys. 05 (2010) E01; M. B. Gavela, L. Lopez Honorez, O. Mena, and S. Rigolin, Dark coupling and gauge invariance, J. Cosmol. Astropart. Phys. 11 (2010) 044.

[42] V. Salvatelli, A. Marchini, L. Lopez-Honorez, and O. Mena, New constraints on coupled dark energy from the Planck satellite experiment, Phys. Rev. D **88**, 023531 (2013).

[43] A. G. Riess, L. Macri, S. Casertano, H. Lampeitl, H. C. Ferguson, A. V. Filippenko, S. W. Jha, W. Li, and R. Chornock, A 3% solution: Determination of the Hubble constant with the Hubble Space Telescope and Wide Field Camera 3, Astrophys. J. **730**, 119 (2011); Erratum, Astrophys. J. **732**, 129(E) (2011).

[44] M. Doran, C. M. Muller, G. Schafer, and C. Wetterich, Gauge-invariant initial conditions and early time perturbations in quintessence universes, Phys. Rev. D **68**, 063505 (2003).

[45] E. Majerotto, J. Valiviita, and R. Maartens, Adiabatic initial conditions for perturbations in interacting dark energy models, Mon. Not. R. Astron. Soc. **402**, 2344 (2010).

[46] G. Ballesteros and J. Lesgourgues, Dark energy with non-adiabatic sound speed: initial conditions and detectability, J. Cosmol. Astropart. Phys. 10 (2010) 014.

[47] N. Aghanim *et al.* (Planck Collaboration), Planck 2015 results. XI. CMB power spectra, likelihoods, and robustness of parameters, Astron. Astrophys. **594**, A11 (2016).

[48] P. A. R. Ade *et al.* (Planck Collaboration), Planck 2015 results. XV. Gravitational lensing, Astron. Astrophys. **594**, A15 (2016).

[49] F. Beutler, C. Blake, M. Colless, D. Heath Jones, L. Staveley-Smith, L. Campbell, Q. Parker, W. Saunders, and F. Watson, The 6dF Galaxy Survey: Baryon acoustic oscillations and the local Hubble constant, Mon. Not. R. Astron. Soc. **416**, 3017 (2011).

[50] A. J. Ross, L. Samushia, C. Howlett, W. J. Percival, A. Burden, and M. Manera, The clustering of the SDSS DR7 main galaxy sample I: A 4 per cent distance measure at $z = 0.15$, Mon. Not. R. Astron. Soc. **449**, 835 (2015).

[51] L. Anderson *et al.* (BOSS Collaboration), The clustering of galaxies in the SDSS-III Baryon Oscillation Spectroscopic Survey: Baryon acoustic oscillations in the Data Releases 10 and 11 Galaxy samples, Mon. Not. R. Astron. Soc. **441**, 24 (2014).

[52] M. Betoule *et al.* (SDSS Collaboration), Improved cosmological constraints from a joint analysis of the SDSS-II and SNLS supernova samples, Astron. Astrophys. **568**, A22 (2014).

[53] A. Lewis and S. Bridle, Cosmological parameters from CMB and other data: A Monte Carlo approach, Phys. Rev. D **66**, 103511 (2002).

[54] A. Lewis, Efficient sampling of fast and slow cosmological parameters, Phys. Rev. D **87**, 103529 (2013).

[55] R. Trotta, Bayes in the sky: Bayesian inference and model selection in cosmology, Contemp. Phys. **49**, 71 (2008).

[56] R. Trotta, Applications of Bayesian model selection to cosmological parameters, Mon. Not. R. Astron. Soc. **378**, 72 (2007).

[57] I. Verdinelli and L. Wasserman, Computing bayes factors using a generalization of the savage-dickey density ratio, J. Am. Stat. Assoc. **90**, 614 (1995).